Index-profile design for low-loss crossed multimode waveguide for optical printed circuit board

Takaaki Ishigure,[1,3] Keishiro Shitanda,[2,4] and Yutaro Oizmi[2,5]

[1] *Faculty of Science and Technology, Keio University, 3-14-1 Hiyoshi, Kohoku-ku Yokohama, 223-8522, Japan*
[2] *Graduate School of Science and Technology, Keio University, 3-14-1 Hiyoshi, Kohoku-ku Yokohama, 223-8522, Japan*
[3] *ishigure@appi.keio.ac.jp*
[4] *lynton@keio.jp*
[5] *oz-music9861@keio.jp*

Abstract: We present an index profile design for remarkably low loss multimode optical crossed waveguide. In this paper, we theoretically calculate the light propagation loss in crossed waveguides with step-index (SI) and graded-index (GI) square cores utilizing a ray tracing simulation. In this simulation, we focus on the index exponent values for the GI profile, which allows low crossing loss even if the number of crossing is as large as 50 or even if the crossing angle is as low as 20°. It is revealed that an index exponent of 2.0 for the GI core strongly contributes to exhibit 35 times lower loss (0.072 dB after 50-perpendicular crosses) compared to the loss of the SI-core counterpart (2.58 dB after the same crossings). The GI cores with a smaller index exponent exhibit better loss in crossed waveguides with a wide range of crossing angles from 30° to 90°. Furthermore, we discuss the effect of the refractive index profile at the intersection on the optical loss of crossed waveguides.

OCIS codes: (130.5460) Polymer waveguides; (080.5692) Ray trajectories in inhomogeneous media; (200.4650) Optical interconnects.

References and links

1. http://www.top500.org/
2. A. Benner, "Optical interconnect opportunities in supercomputers and high end computing," in *Optical Fiber Communication Conference and Exposition* 2012, Paper OTu2B4.
3. F. E. Doany, C. L. Schow, B. G. Lee, R. A. Budd, C. W. Baks, C. K. Tsang, J. U. Knickerbocker, R. Dangel, B. Chan, H. Lin, C. Carver, J. Haung, J. Berry, D. Bajkowski, F. Libsch, and J. A. Kash, "Terabit/s-class optical PCB links incorporating 360-Gb/s bidirectional 850 nm parallel optical transceivers," J. Lightwave Technol. **30**(4), 560–571 (2012).
4. R. C. A. Pitwon, K. Wang, J. Graham-Jones, I. Papakonstantinou, H. Baghsiahi, B. J. Offrein, R. Dangel, D. Milward, and D. R. Selviah, "FirstLight: Pluggable optical interconnect technologies for polymeric electro-optical printed circuit boards in data centers," J. Lightwave Technol. **30**(21), 3316–3329 (2012).
5. N. Bamiedakis, A. Hashim, R. V. Penty, and I. H. White, "A 40 Gb/s optical bus for optical backplane interconnections," J. Lightwave Technol. **32**(8), 1526–1537 (2014).
6. N. Bamiedakis, J. Beals, R. V. Penty, I. H. White, J. V. DeGroot, and T. V. Clapp, "Cost-effective multimode polymer waveguides for high-speed on-board optical interconnects," J. Quantum Electron. **45**(4), 415–424 (2009).
7. F. Betschon, M. Michlerb, D. Craiovanc, M. Halter, K. Dietrichb, J. Kremmelb, J. F. M. Gmür, and S. Paredes, "Mass production of planar polymer waveguides and their applications," Proc. SPIE **7607**, 76070M (2010).
8. T. Ishigure and Y. Takeyoshi, "Polymer waveguide with 4-channel graded-index circular cores for parallel optical interconnects," Opt. Express **15**(9), 5843–5850 (2007).
9. Y. Takeyoshi and T. Ishigure, "High-density 2×4 channel polymer optical waveguide with graded-index circular cores," J. Lightwave Technol. **27**(14), 2852–2861 (2009).
10. K. Soma and T. Ishigure, "Fabrication of a graded-index circular-core polymer parallel optical waveguide using a microdispenser for a high-density optical printed circuit board," IEEE J. Sel. Top. Quantum Electron. **19**(2), 3600310 (2013).

#243355 Received 19 Jun 2015; revised 5 Aug 2015; accepted 7 Aug 2015; published 14 Aug 2015

11. C. Jian, N. Bamiedakis, T. J. Edwards, C. T. A. Brown, R. V. Penty, and I. H. White, "Dispersion studies on multimode polymer spiral waveguides for board-level optical interconnects," in *Proceedings of IEEE Optical Interconnects Conference* (IEEE, 2015), pp. 26–27.
12. B. W. Swatowski, C. M. Amb, M. G. Hyer, R. S. John, and W. K. Weidner, "Graded index silicone waveguides for high performance computing," in *Proceedings of IEEE Optical Interconnects Conference* (IEEE, 2014), pp. 133–134.
13. T. Okoshi, *Optical Fibers* (Academic Press, 1982), Chapter 3.
14. A. W. Snyder and J. D. Love, *Optical Waveguide Theory* (Chapman and Hall, 1995), Part I.
15. T. Mori, K. Takahama, M. Fujiwara, K. Watanabe, H. Owari, Y. Shirato, S. Terada, M. Sakamoto, and K. Choki, "Optical and electrical hybrid flexible printed circuit boards with unique photo-defined polymer waveguide layers," Proc. SPIE **7607**, 76070S (2010).
16. R. Olshansky and D. B. Keck, "Pulse broadening in graded-index optical fibers," Appl. Opt. **15**(2), 483–491 (1976).
17. T. Ishigure and Y. Nitta, "Polymer optical waveguide with multiple graded-index cores for on-board interconnects fabricated using soft-lithography," Opt. Express **18**(13), 14191–14201 (2010).
18. T. Mori, K. Moriya, K. Kitazoe, S. Takayama, S. Terada, M. Fujiwara, K. Takahama, K. Choki, and T. Ishigure, "Polymer optical waveguide having unique refractive index profiles for ultra high-density interconnection," in *Optical Fiber Communication Conference and Exposition* 2012, Paper OTu1I6.
19. T. Ishigure, K. Shitanda, T. Kudo, S. Takayama, T. Mori, K. Moriya, and K. Choki, "Low-loss design and fabrication of multimode polymer optical waveguide circuit with crossings for high-density optical PCB," *in Proceedings of Electronics Components and Technology Conference*, 297–304 (2013).
20. P. Pepeljugoski, S. E. Golowich, A. J. Ritger, P. Kolesar, and A. Risteski, "Modeling and simulation of next-generation multimode fiber links," J. Lightwave Technol. **21**(5), 1242–1255 (2003).

1. Introduction

The performance gain of microprocessors has been accelerating the arithmetic processing speed of high performance computers (HPCs), which has led to a worldwide performance competition amongst HPCs [1]. For sustaining the growth of the HPCs' ever-increasing performance, the power consumption of HPC systems will become a critical issue. Therefore, optical wiring is gradually being introduced into such HPC systems.

Currently, some HPCs with greater than peta FLOPS performance already have adopted multimode optical fiber (MMF) links for their rack-to-rack data exchanges, where optical/electrical (O/E) and E/O signal conversions take place at the edge of a printed circuit board (PCB). In advanced systems, the O/E and E/O conversions are required to be very close to the processor chips, because the signal distortion in the on-board electrical wiring (even in such a short link) should be reduced for further high-speed and power-efficient operations [2]. Optical PCBs (O-PCBs) have been a promising solution to realize on-board optical interconnects, by which wiring density much higher than multimode fiber links mentioned above can be realized.

Hence, O-PCBs incorporating polymeric optical waveguides have been drawing much attention, because of their ease of fabrication, good miscibility with PCB substrates, and low cost [3–5]. For realizing O-PCBs, polymer waveguides with just straight cores have been intensively developed worldwide. Meanwhile, curved waveguides and crossed waveguides are highly anticipated for wiring on-board. In particular, crossed optical waveguides with low loss and low interchannel crosstalk allow single-layer optical wirings on PCBs, which would lead to a flexible structural design. In fact, research into crossed polymer waveguides, which are normally based on existing polymer optical waveguides with SI cores has become more active over the last couple of years [6, 7]. However, the excess optical loss at the intersection of two cores due to the light leakage has been crucial. Meanwhile, we have demonstrated that multimode polymer waveguides with graded-index (GI) core show lower loss, lower interchannel crosstalk, and lower connection loss with multimode optical fibers with a circular GI core [8–10]. Thanks to that research, GI-core polymer waveguides have been drawing attention [11, 12]. However, it has not yet been discussed how the index profile, a very important characteristic of GI-core contributes to low-loss waveguides.

In this paper, we focus on the optical loss of crossed multimode waveguides, and, propose a new crossed waveguide composed of GI-cores. The loss at the intersection in the crossed cores is theoretically calculated using a ray-trace simulation.

#243355 Received 19 Jun 2015; revised 5 Aug 2015; accepted 7 Aug 2015; published 14 Aug 2015

2. Theoretical analysis of light propagation

2.1 Ray-trace method

A lot of analytical methods have been proposed for simulating the lightwave propagation in optical waveguides. The analyses based on wave optics like the beam propagation method (BPM) and the finite-difference time-domain method (FDTD) have been used frequently over the last decade. However, the GI-core multimode crossed waveguides which are the focus of this paper have a large number of core intersections, and the refractive index profile in the intersection could be different from that at the straight region of the cores. Therefore, waveguide structural variations exist both in the lateral and axial directions. Furthermore, the polymer waveguides in this paper have a numerical aperture (NA) as high as 0.25 and a core size as large as 50 μm. These features could make the wave-optics based simulation more complicated and difficult, resulting in a longer computation time. Hence, in this paper, we adopt the ray tracing method for the simulation. It is well known that a high degree of accuracy can be obtained by ray tracing methods, particularly for multimode waveguides [13]. In addition, the axial variation of the index profiles mentioned above is less influential on the computation time in the ray tracing simulation.

The light propagation in graded-index medium is expressed by the ray equation as follows [14]

$$\frac{d}{ds}\left[n(\boldsymbol{r})\frac{d\boldsymbol{r}}{ds} \right] = \nabla\{n(\boldsymbol{r})\} \tag{1}$$

where, $n(\boldsymbol{r})$ is the refractive index at the position vector $\boldsymbol{r}$, and, s is the distance along the ray path. In this paper, the refractive index profiles in rectangular-shaped cores are approximated by a modified power-law form as shown by Eqs. (2) to (5):

$$n(x,y) = n_{co}\left[1-2\Delta\{f(x)+g(y)\}\right]^{\frac{1}{2}} \tag{2}$$

$$f(x)=\left|\frac{x}{a_x}\right|^{p},\ g(y)=\left|\frac{y}{a_y}\right|^{q},\ \Delta=\frac{n_{co}^2-n_{cl}^2}{2n_{co}} \tag{3}$$

When

$$f(x)+g(y)\geq 1, \tag{4}$$

$$n(x,y) = n_{cl} \tag{5}$$

Here, n_{co} and n_{cl} are the refractive indices at the core center and the cladding, respectively, while a_x and a_y are the half-width and the half-height of the rectangular core, respectively. Two index exponents, p and q express the index profiles in the horizontal and vertical directions in the core, respectively.

2.2 Calculation condition

For the crossed waveguide simulation, we apply the above approximated index profiles to the program. Figure 1 shows the structure of *perpendicularly* crossed waveguide that we focus in this paper. Here, n_{co} and n_{cl} are set to be 1.553 and 1.536, respectively, supposing a poly norbornene based waveguide developed at Sumitomo Bakelite Co., Ltd [15]. The index profile in the core is varied by the index exponents, p and q in the horizontal (x-) and vertical (y-) directions, respectively. Here, for approximating an SI core by the power-law form, we generally apply infinity to the index exponent [16]. However, we preliminary confirmed that when p and q are as high as 40, the rays in the core show trajectories very close to the total internal reflection, which is seen in SI cores. Hence, we apply the condition of $p = q = 40$ for the *straight region* in the SI-core crossed waveguide in the ray trace simulation. Here, as

#243355 Received 19 Jun 2015; revised 5 Aug 2015; accepted 7 Aug 2015; published 14 Aug 2015

shown in Fig. 1, we call the core regions between two intersections the "straight core (region)." So, the same simulation program could be used for the simulation on SI and GI cores by just setting the parameters p and q.

Meanwhile, when we apply the fabrication techniques for experimentally obtaining "GI-core" polymer waveguides, such as the soft-lithography method [17] or the photo-addressing method [18] to the crossed waveguides, the diffusion of the core material into the cladding (and vice versa) plays a key role. A concentration distribution formed after the diffusion of core and cladding materials finally corresponds to a GI profile. In the case of crossed waveguides, it is difficult to expect the monomer diffusion in the intersection area to be the same as that in the straight cores, because no cladding exists in both x- and z-directions. Therefore, for the simulation, all the intersections are assumed to have an SI profile (n_{int}) in "both SI- and GI-core" crossed waveguides, which should be the worst case for the GI-core crossed waveguide.

In the following sections, we simulate the optical loss from crossed waveguides and discuss the low-loss waveguide design. First, the core sizes a_x and a_y shown in Fig. 1 are set to be $2a_x = 2a_y = 50$ μm. As mentioned above, ray tracing methods are applicable to such large-core multimode waveguides with a high accuracy. The waveguides include 50 perpendicular crossings with a pitch P and a distance P_{in} from the input end to the first intersection, as shown in Fig. 1. Here P and P_{in} are set to 250 and 125 μm, respectively. It is well known that the launching condition is a very important issue for multimode waveguide characteristics. We define the condition by setting the spot size (beam waist) 2ε of the incident beam to be 10 μm, supposing a vertical cavity surface emitting laser (VCSEL) based light source emitting at a wavelength of 850 nm. Then, we let each incident ray to have a different optical intensity. The total number of input rays is 10,000, by realizing a Gaussian near-field pattern (NFP) with a 10-μmø beam waist. Meanwhile, the input numerical aperture (NA) of the ray bundle is set to be 0.20, slightly lower than the NA of the waveguide. Here, we suppose the total angular intensity profile of the injected rays to be a Gaussian, as well. The dependence of the launching condition on the loss is evaluated in the next section.

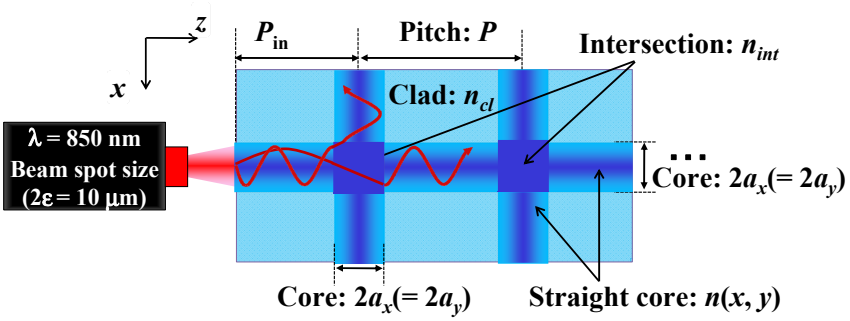

Fig. 1. Model structure of crossed waveguides for simulation.

3. Calculated property of crossed waveguide

3.1 Optical loss due to crossing structure

The optical losses of the crossed waveguides are statistically analyzed by accumulating the intensity of all the rays that pass through the crossings. As mentioned above, the refractive index of the intersection (n_{int}) is flat, and n_{int} is set to be identical to n_{co}, as described by Eq. (2) in both SI-core and GI-core crossed waveguides. Figure 2 shows the results we previously reported [19]. Here, the total (accumulated) loss due to the crossings is plotted with respect to the number of crossing for the SI- and GI-core crossed waveguides. The conditions on the index exponents $p = q = 40$ and $p = q = 3$ are applied to the simulations on SI and GI cores, respectively only in those straight regions.

#243355 Received 19 Jun 2015; revised 5 Aug 2015; accepted 7 Aug 2015; published 14 Aug 2015

The total loss of the SI-core crossed waveguide after 50 crossings is calculated to be 2.58 dB, which is almost 25 times higher than the loss of the GI-core (with $p = q = 3$) crossed waveguide (0.0958 dB) after the same number of crossing. In the case of SI-core waveguides, the existence of cladding is required for the total internal reflection. At the intersection in SI-core crossed waveguides, some rays could leak to the crossed core, as illustrated in Fig. 3(a), because the cladding does not exist in the x-axis direction. Contrastingly, the cladding is not necessarily required for the rays in the GI core to propagate to the z-axis direction, because these rays are confined in the core due to the refraction. In GI cores with $p = q = 2$, it is well known that the rays propagate with a sinusoidal trajectory [14]. When we focus on the meridional rays, the angle between a ray and the core axis is the maximum when the ray passes over the core center axis, while when the ray approaches to the core-cladding boundary, the ray direction turns into parallel to the z-axis. Therefore, in the GI-core crossed waveguides, very few rays leak to the crossed core at the intersections, as shown in Fig. 3(b). In Fig. 2, the experimentally measured loss for a GI-core crossed waveguide is compared [19], which shows remarkably low values as calculated, but they are even lower than the simulated result.

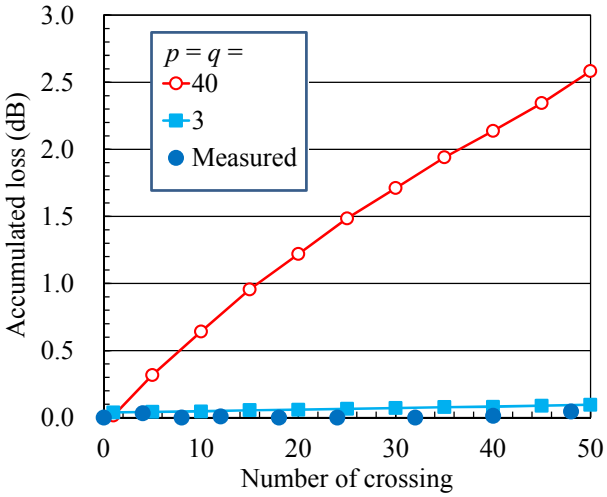

Fig. 2. Calculated optical loss from SI- and GI-core crossed waveguides.

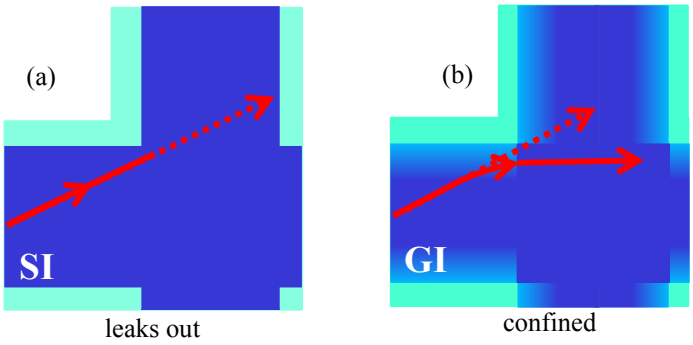

Fig. 3. Difference of ray trajectory between SI- and GI-core crossed waveguides.

3.2 Effects of refractive index at intersection and core size

For calculating the results in Fig. 2, we assume that the intersections in the GI-core crossed waveguide have a uniform refractive index ($n_{int} = n_{co}$). So, in the GI-core crossed waveguide,

#243355 Received 19 Jun 2015; revised 5 Aug 2015; accepted 7 Aug 2015; published 14 Aug 2015

the difference of the refractive indices at the straight and the intersection regions could affect the waveguide loss. The rays are refracted at the boundary between the straight and intersection regions, following Snell's law, as shown in Fig. 3(b). Because of the gradual lateral decrease of the refractive index from the core center, the refraction angle (the angle between the ray direction and waveguide axis) of the ray is smaller with increasing distance between the core center and the point at which the ray injects into the intersection. Thus, the ray is more likely to confine in the core, even if it is injected into an intersection at a position near the cladding.

Therefore, the dependence of the loss of the GI-core crossed waveguide on the value of n_{int} is simulated. For the calculation, n_{int} is varied from n_{co} to n_{cl}, and the results when n_{int} is 1.553, 1.545, and 1.536 are shown in Fig. 4(a). Other simulation conditions except for the n_{int} setting are the same as those for the results in Fig. 2. From Fig. 4(a), although it is found that higher n_{int} shows lower loss, after 50 crossings, only 0.02-dB higher loss is observed, even if n_{int} has the lowest value, n_{cl}. When n_{int} equals n_{cl}, the refraction angle of the ray at the boundary of straight region and the intersection is larger than the incident angle, which could lead to the ray leaking. However, since the difference between $n(x, y)$ and n_{cl} is quite small, the refracted ray can still remain confined in the core. Thus, despite the SI profiles at all the intersections, the strong optical confinement effect of GI cores plays a key role for reducing the ray leakage.

Meanwhile, the intersection with a uniform refractive index, n_{int} could cause Fresnel reflection loss. As mentioned above, the index difference between $n(x, y)$ and n_{int} is very small, and the largest incident angle of a ray to the intersection is calculated to be as small as 8° to 10° from the NA value of the waveguide. Because of these reasons, the loss due to Fresnel reflection should be as low as 0.007 dB for 50 crossings at highest. Thus, even if the loss due to Fresnel reflection is taken into account, the crossing loss in GI-core crossed waveguides is still low enough.

In the ray trace simulation, the core size could be another concern that the calculated results could be over or under estimated. Hence, the core size dependence of the loss in the GI-crossed waveguide is also simulated. The core width and height, $2a_x$, $2a_y$ are varied to be 35, 50, 75, and 100 μm. Even though the core size is varied, the values of P and P_{in} in Fig. 1 are fixed, and other simulation conditions are identical to those for the results in Fig. 2. The results are shown in Fig. 4(b). Although approximately 0.04-dB loss difference is observed between the results of 50-μm and 100-μm core size after 50 crossings, there is no clear core size dependence. For those ray trace simulations, the total number of injected ray is 10,000, and the direction and intensity of each ray is determined using a random number, following the Monte Carlo method. The influence of the deviation of launching conditions due to the random number usage is calculated to be ± 0.03 dB after 50 crossings when $p = q = 3$, while it is ± 0.05 dB when $p = q = 40$. Therefore, the loss dependences on n_{int} and core size shown in Figs. 4(a) and 4(b) could include this fluctuation due to the random number usage. Thus, even under the adverse conditions for GI core, the crossing losses are low enough compared to the SI-core crossed waveguide. In the results shown in Figs. 4(a) and 4(b), it is interesting that the highest loss increment is observed at the first crossing, followed by gradual loss increase. In addition, periodical abrupt loss increments are observed. Since the higher order modes are likely to leak preferentially, the large loss increment at the first crossing is understandable. Meanwhile, the cause of this periodical loss increase is discussed in section 3.5.

#243355 Received 19 Jun 2015; revised 5 Aug 2015; accepted 7 Aug 2015; published 14 Aug 2015

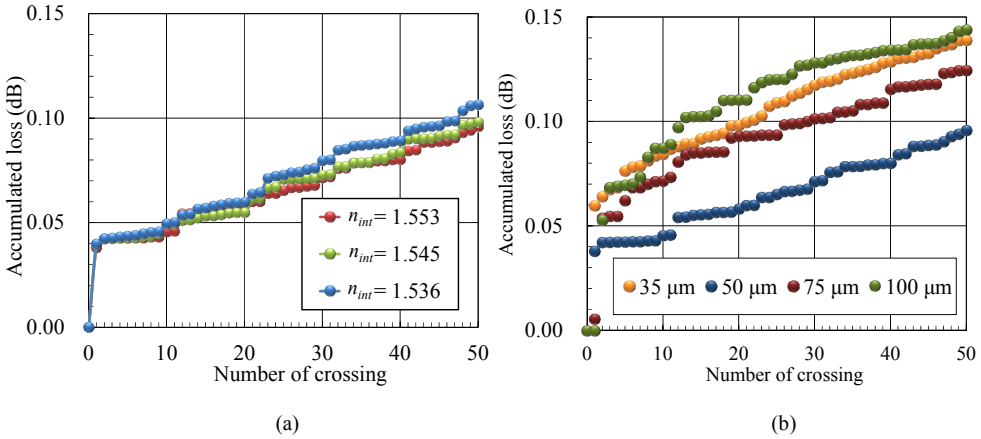

Fig. 4. Crossing loss dependence on (a) the refractive index (n_{int}) at the intersection and (b) core size.

3.3 Index profile dependence

In the above sections, we simulate the loss of the GI-core crossed waveguide with the index exponents $p = q = 3$, although it is well known that the condition of $p = q = 2$ should be ideal from the modal dispersion point of view. After we published the simulated results [19], other ways to fabricate GI-core crossed waveguides have been investigated [12]. However, the index profile looks deviated from a parabolic shape, and even asymmetric. That means it is difficult to precisely control the refractive index profile to have a unique value of p and q when we apply the actual fabrication procedures. In most fabrication techniques for GI-cores, the diffusion of core and cladding materials is important for controlling the refractive index profile, and thus it would be much more difficult to form an index profile with $p = q = 2$ than that with larger values of p and q. Therefore, in this section, we focus on the crossing loss dependence on the index profiles at the straight region.

In Fig. 5(a), the simulated results of the accumulated crossing loss from a perpendicularly crossed waveguide is indicated with respect to the crossing number. In this calculation, the parameters p and q for the straight region are varied as $p = q = 2$, 5, 7, 10 and 40. In these cases, the difference in the refractive index profiles is confirmed from Fig. 6. It is found from Fig. 5(a) that with increasing the values of p and q, the crossing loss increases. Although a difference of the two index profiles between $p = q = 2$ and $p = q = 5$ are clearly observed in Fig. 6, the accumulated losses of the two profiles are quite low, compared to the case when $p = q = 10$ and larger. Here, the loss values after 20 and 50 crossings are extracted, and these loss values are plotted over the index exponent values (p and q) in Fig. 5(b). It is very interesting that the accumulated crossing loss abruptly increases when the index exponent (p and q) exceeds 5.0, as shown in Fig. 5(b). From these results, we confirm that only a slight index gradation forms at the core-cladding boundary; this reduces the crossing loss, for instance when $p = q = 10$. However, we also verify that the index exponents p and q should be as small as 5 or less for realizing a waveguide with sufficiently low crossing loss, although it strongly depends on the crossed waveguide design: the required number of crossing, crossing angle, etc.

In addition to the variety of index exponents, the difference between the values p and q could be another concern. In the above calculations, we set the parameters p and q to be identical, but in general the p and q could be different when we utilize several techniques for fabricating GI-core waveguides as currently proposed. We preliminary calculated the influence of different p and q, and reported it in [19], but the detailed discussion for such asymmetric index profile ($p \neq q$) will be published elsewhere.

#243355 Received 19 Jun 2015; revised 5 Aug 2015; accepted 7 Aug 2015; published 14 Aug 2015

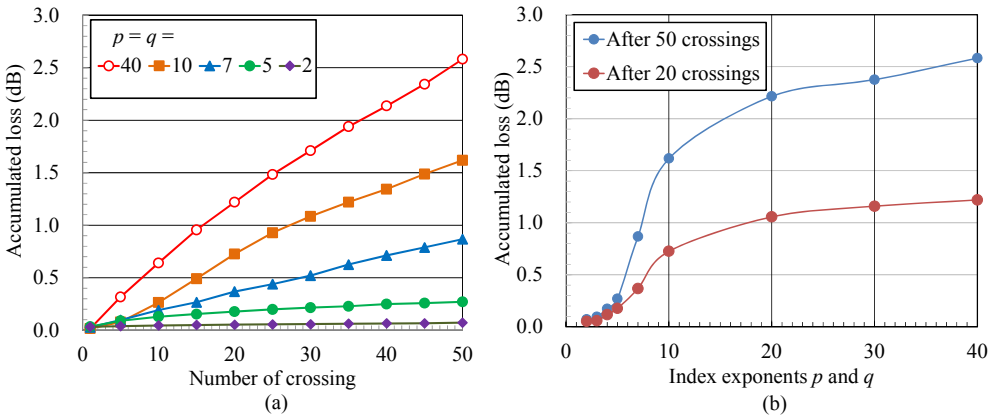

Fig. 5. Accumulated crossing loss dependence on the index exponent (a) with respect to the number of crossing (b) crossing loss comparison after 20 and 50 crossings.

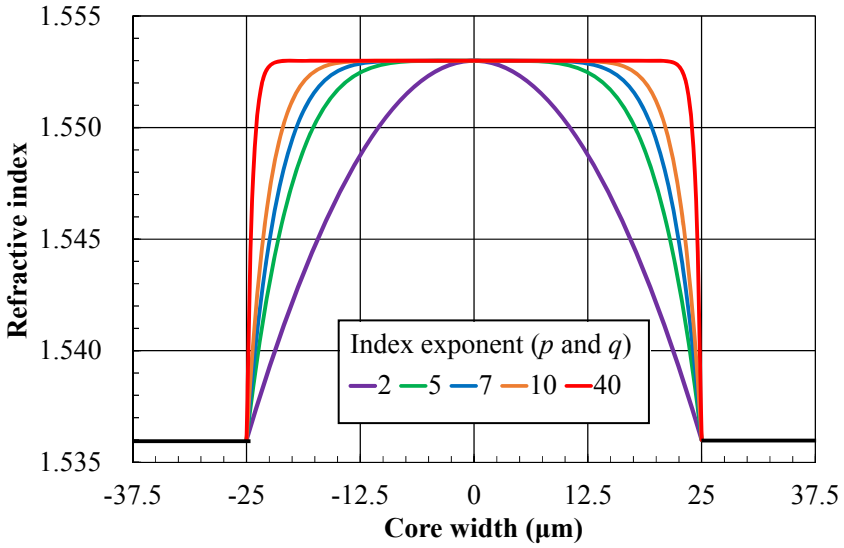

Fig. 6. Variation of refractive index profiles expressed by the power-law form with different index exponent.

3.4 Launch condition

In the above calculations, we theoretically demonstrate that the GI core with index exponents p and q smaller than 5.0 remarkably reduces the crossing loss in perpendicularly crossed waveguides. Furthermore, the low loss in GI-core crossed waveguide is sustained even if the intersection region has an SI profile. Here, since the waveguides under discussion propagate as multimode, it is important to note that the optical characteristics largely depend on the launching condition. As explained in 2.2, we define the input light beam composed of multiple rays with a Gaussian intensity with a 10-μm spot size, and a Gaussian angular distribution to have a launch NA of 0.20. This launch condition might be regarded as being advantageous for the GI-core crossed waveguides. Therefore, in this section, we investigate the crossing loss dependence of both SI- and GI-core crossed waveguides on the launch condition: spot size and offset.

#243355 Received 19 Jun 2015; revised 5 Aug 2015; accepted 7 Aug 2015; published 14 Aug 2015

Figure 7 shows the simulated results when the spot size is set to be 30 μm and 40 μm, comparing to the results with a 10-μm spot size. We observe little influence of the spot size on the accumulated loss. In the case of GI-core waveguides, if the rays are injected to the core at a point apart from the core center, the rays frequently pass through the periphery of the core as high order modes. So, these rays might tend to leak to the crossed cores. That means the larger spot size could lead to high loss even in the GI crossed waveguide. Indeed, in the case when $p = q = 5$ and lower, the loss increases with increasing spot size, while no clear spot size dependence is found in the SI-core waveguide ($p = q = 40$). However, it is found that the spot size of the launch beam is not crucial to cause the crossing loss as high as the loss observed in the SI-core crossed waveguide.

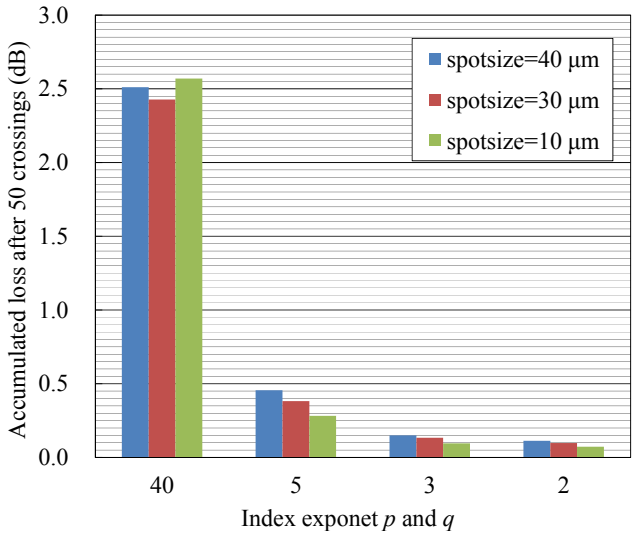

Fig. 7. Accumulated crossing loss of SI- and GI-core crossed waveguides after 50 crossings with respect to the launch beam spot size.

Meanwhile, the offset launch is widely used for intentionally exciting higher order modes in GI MMF for measuring the differential mode delay [20]. Hence, it is a concern particularly in GI-core crossed waveguides that the crossing loss increases under the offset launch condition. The calculated losses after 50 crossings in SI- and GI-core crossed waveguides under offset launch conditions are shown in Fig. 8. For this simulation, the position of incident beam to the waveguides is shifted in the *x*-direction shown in Fig. 1 with a 5-μm step, and then the crossing loss is calculated. Here, a coupling loss is caused under an offset launch condition, particularly in the GI-core waveguide. To obtain the crossing loss, the coupling loss is subtracted, so the "accumulated loss" in Fig. 8 is the optical loss simply caused by the core crossings. As shown in Fig. 8, the loss as high as 2.5 dB in the SI core at 0-μm offset is observed consistently even under the offset conditions. In the SI core, the ray trajectory exhibits little change under offset launch conditions compared to the center launch: the incident angle is the only parameter which affects whether the ray leaks or not. Contrastingly, the crossing loss from the GI-core waveguide slightly increases with increasing the offset. However, even if a 15-μm offset is added, the loss increment is only 0.26 dB, which is still much lower than the loss from the SI counterpart. Although under the 15-μm offset, the higher order modes in GI-core are strongly excited, even such high order modes are tightly confined in the GI core to show extremely low crossing loss.

Thus, the GI-core crossed waveguide exhibits remarkably lower loss than the SI-core counterpart regardless of the launch conditions. In the experimentally fabricated GI-core crossed waveguides, the refractive index at the intersection would not be flat but have a variation. In the case that the n_{int} is no longer flat, it is already found that the crossing loss is

#243355 Received 19 Jun 2015; revised 5 Aug 2015; accepted 7 Aug 2015; published 14 Aug 2015

rather lower [19]. In addition, in all the above simulations, the index profiles in the horizontal and vertical directions are set to be the same ($p = q$). However, in the crossed waveguides experimentally fabricated, these two profiles are not necessarily identical. Indeed, a waveguide fabricated using the photo-addressing method has an asymmetric profile: SI and GI profiles in the vertical and horizontal directions, respectively. We called this profile as SI-GI profile. The calculated loss in the SI-GI core crossed waveguides were already reported in [19], and the detailed influences of asymmetric index profiles on the crossing loss will be described elsewhere as well as the influence of the index profile at the intersection.

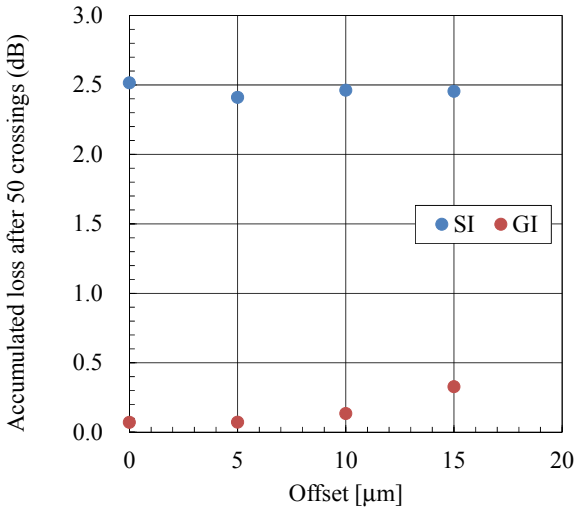

Fig. 8. Influence of offset launch on accumulated crossing loss in the SI- ($p = q = 40$) and GI-core ($p = q = 3$) crossed waveguides.

3.5 Loss mechanism

In the ray trace simulation program, each leaked ray from the core is traced how and from where the ray leaks out. Then, the loss mechanism can be analyzed statistically. The results for SI ($p = q = 40$) and GI ($p = q = 3$) are summarized in Fig. 9. Here, all the leaked rays are classified into three categories: (1) the rays leaked at the intersection, (2) the rays leaked at the straight region, and (3) the rays leaked with other causes, for instance just at the corner (due to ray tracing limit). These three classifications are expressed in Fig. 9 as "intersection," "straight," and "radiation," respectively.

It is noteworthy that the light ray leakage from the core is observed even at the straight region as well as the intersection. In the SI-core crossed waveguide, the largest factor in the ray leakage is the lack of cladding at the intersections, so approximately 70% of leakage occurs at the intersection, as shown in Fig. 9. Contrastingly, more than 90% of ray leakage from GI-core crossed waveguide is observed at the straight region. Most of the rays propagate with a quasi-sinusoidal trajectory in the GI core at straight regions. After they enter into the intersection with a uniform refractive index, they follow straight light paths. Then, the rays enter again into the GI straight region, as illustrated in Fig. 3(b). Here, the exiting points of the rays from the intersection shift slightly compared to their entrance points to the intersection, due to the straight propagation. This shift corresponds to an offset launch for the GI-core next to the intersection, such that the ray converts to a different order mode. Therefore, the intersection with a flat refractive index works as a mode converter in GI-core crossed waveguides. Here, we focus on a ray that initially enters into the waveguide as a low-order mode. After passing through the intersections several times, the ray is converted to a higher-order mode. Even after passing through those intersections, most of the rays can again enter into the next straight region because of the unique ray propagating direction in GI cores

#243355 Received 19 Jun 2015; revised 5 Aug 2015; accepted 7 Aug 2015; published 14 Aug 2015

explained in section 2.1. However, it no longer enters with an incident angle for a propagating mode, and finally it leaks out from the core. This is the reason why most of rays in the GI core leak at the straight region. Therefore, if the intersection region has a GI profile, by which mode conversion is suppressed, much lower crossing loss is realized.

In addition, this ray leakage mechanism which is very specific in GI cores could be one of the reasons why a periodical abrupt increase in loss is observed in Fig. 4. Although the incident angles and intensities of injected rays are randomly defined in the program, the random number is not necessarily random. So, rays could be classified into a "mode group," and the rays involved in the same mode group leak simultaneously after passing a certain number of crossings, resulting in abrupt loss increment. In the experimentally measured crossing loss in the GI crossed waveguide in Fig. 2, such a periodical loss increment is not necessarily observed. Hence, the assumption of a uniform refractive index at the intersection is not accurate in the actual waveguide samples. The index profiles in the intersection should be evaluated in more detail.

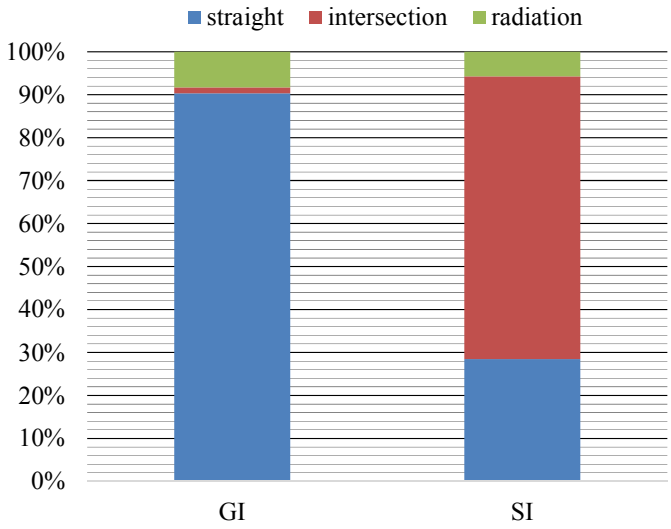

Fig. 9. Classification of ray-leakage point in GI- and SI-core crossed waveguides.

3.6 Crossing angle dependence

For the O-PCB applications, a more flexible waveguide structure is required in addition to perpendicularly crossed waveguides, which means the crossing angle of cores are not limited to 90°. With decreasing the crossing angle, the rays could be more likely to leak. Therefore, the crossing angle dependence of the waveguide loss is calculated. A relationship between the average waveguide loss per crossing and crossing angle is shown in Fig. 10. The average waveguide loss is obtained from the accumulated loss of the crossed waveguide after 50 crossings. We observe a quite interesting result that even if the crossing angle is smaller than 90°, the light leakage is sufficiently low in the GI core than in SI core over a wide range of crossing angles. In the above section, we mention that an index exponent smaller than 5 is required for sufficiently low crossing loss particularly in perpendicularly crossed waveguide. However, in the case when $p = q = 5$ and higher, the crossing angle dependence is large, while in the waveguides with a smaller index exponent, the low crossing loss at a 90° angle is sustained over a wide range of crossing angles down to 50°. Hence, it is confirmed that GI-core crossed waveguides have a great superiority for reducing the crossing loss. In particular, GI-core waveguides with an index profile very close to parabolic shape ($p = q = 2$) have a large advantage in decreasing the loss over a wide variety of crossing structures.

#243355 Received 19 Jun 2015; revised 5 Aug 2015; accepted 7 Aug 2015; published 14 Aug 2015

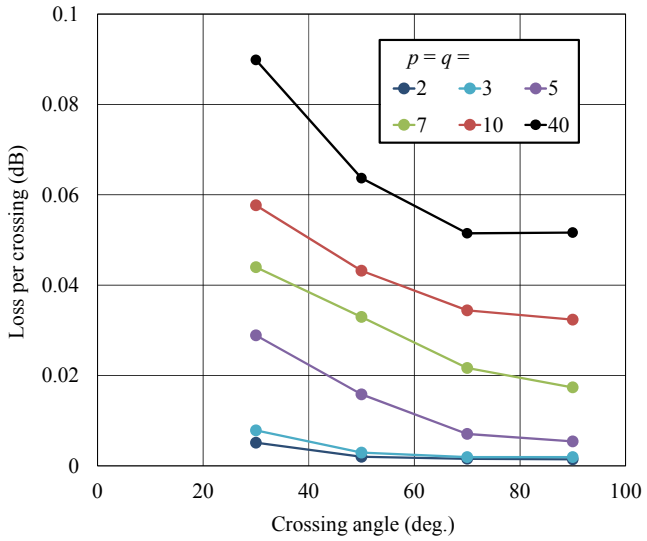

Fig. 10. Crossing angle dependence of SI- and GI-core crossed waveguides.

4. Conclusion

In this paper, we designed the index profile for multimode crossed waveguide to exhibit a low crossing loss, using a ray tracing method. The tight optical confinement effect of the GI core allows a significant reduction of excess optical loss due to core crossing compared to the SI-core counterpart (2.58 dB to 0.072 dB for 50 crossings, corresponding to 0.05 dB/cross and 0.0015 dB/cross, respectively), even if the refractive index profile at the intersection is not the same GI structure but an SI profile. It was also found that the rays in SI-core crossed waveguides leaked out mainly at the intersection, because of the lack of cladding. Meanwhile, the rays entered into GI-core crossed waveguides were essentially confined in the core, and few rays leaked at the intersection. In particular, if the intersection has a uniform refractive index (SI profile), the intersection works as a mode converter: the propagating modes (rays) are converted to leaky modes (rays) after passing several crossings.

For realizing very low loss crossed waveguides, a GI profile close to parabolic shape is a desirable profile. Hence, the GI-core multimode waveguides will pave the way for high-bandwidth density on-board optical interconnects.

Acknowledgments

This work is partially supported by the New Energy and Industrial Technology Development Organization (NEDO), project code: P12004.

#243355 Received 19 Jun 2015; revised 5 Aug 2015; accepted 7 Aug 2015; published 14 Aug 2015